

# Fully Automated Image Preprocessing for Feature Extraction from Knife-edge Scanning Microscopy Image Stacks

## Towards a Fully Automated Image Processing Pipeline for Light Microscopic Images

Shruthi Raghavan and Jaerock Kwon

Department of Electrical and Computer Engineering,  
Kettering University, 1700 University Ave., 48504, Flint, MI, U.S.A.

Keywords: KESM, Artifact Removal, Preprocessing, Tissue Extraction, Image Normalization.

Abstract: Knife-Edge Scanning Microscopy (KESM) stands out as a fast physical sectioning approach for imaging tissues at sub-micrometer resolution. To implement high-throughput and high-resolution, KESM images a tissue ribbon on the knife edge as the sample is being sectioned. This simultaneous sectioning and imaging approach has following benefits: (1) No image registration is required. (2) No manual job is required for tissue sectioning, placement or microscope imaging. However spurious pixels are present at the left and right side of the image, since the field of view of the objective is larger than the tissue width. The tissue region needs to be extracted from these images. Moreover, unwanted artifacts are introduced by KESM's imaging mechanism, namely: (1) Vertical stripes caused by unevenly worn knife edge. (2) Horizontal artifacts due to vibration of the knife while cutting plastic embedded tissue. (3) Uneven intensity within an image due to knife misalignment. (4) Uneven intensity levels across images due to the variation of cutting speed. This paper outlines an image processing pipeline for extracting features from KESM images and proposes an algorithm to extract tissue region from physical sectioning-based light microscope images like KESM data for automating feature extraction from these data sets.

## 1 INTRODUCTION

Analysis of biological structures in tissues at sub micrometer resolution is enabled by techniques like the Knife Edge Scanning Microscopy (KESM) (Mayerich et al., 2008), Confocal Microscopy (Shotton, 1989), Automatic tape collecting lathe ultramicrotome (ATLUM) (Hayworth et al., 2006), Serial Block Face Scanning Electron Microscopy (SBFSEM) (Denk and Horstmann, 2004) and All Optical Histology (Tsai et al., 2003). These microscopic imaging methods are based on either physical or optical sectioning, or both (ATLUM).

Knife-edge scanning microscopy is the technique of concurrently slicing and imaging tissue samples at sub micrometer resolution. This preserves image registration throughout the depth of the tissue block and eliminates undesirable events such as back-scattering of light and bleaching of fluorescent-stained tissue below the knife.

The KESM based high-throughput and high-resolution tissue scanner has produced multiple

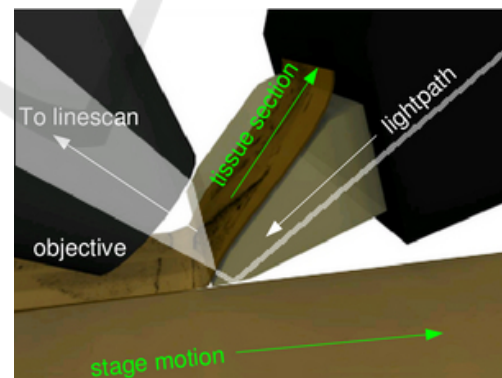


Figure 1: Imaging principles of the KESM. The objective and the knife is held in place, while the specimen affixed on the positioning stage moves at the resolution of 20 nm and travel speed of 1-5, and gets scraped against the diamond knife (5 mm wide for 10X objective), generating a thin section flowing over the knife. Imaging happens at knife-edge. Direction of movement of light and stage is indicated with solid arrows. (Adopted from (Choe et al., 2011)).

datasets till date. A diamond knife is used as collimator and also to section the tissue as illustrated in

Figure 1. The tissue sample being sliced by the knife is imaged just above the knife edge by a powerful line scan camera. The image capture mechanism is triggered based on the encoded position of the tissue being sliced, which ensures that every sectioning results in an image capture. The KESM can image a  $1\text{cm}^3$  tissue block in approximately 50 hours at a resolution of  $0.6\mu\text{m} \times 0.7\mu\text{m} \times 1.0\mu\text{m}$ .

To get information from this data, the KESM images have to be preprocessed followed by feature extraction and post-processing if necessary. This paper describes the first preprocessing step in an image processing pipe that is being designed for automating feature extraction and sharing. A novel method for extraction of tissue regions is being proposed for physical sectioning-based light-microscope imaging data.

## 2 BACKGROUND

While sectioning and imaging in KESM, width of the tissue slice is not exactly the field of view of the objective. Thus, there is additional non-tissue area that appears as dark regions on either side of the tissue in every image. The additional region causes significant increase in the amount of memory required by applications that process the images. For instance, assume we imaged a tissue sample using KESM. Let the width of a line scan image be 4096 pixels and a slice consist of 12000 lines. If pixels are a byte each, the raw KESM image will occupy 46.875MB. However, if tissue width is only 2400pixels, only 27.466MB of memory is actually useful. KESM could collect terabytes of images and 41.41% reduction in image size will significantly improve the efficiency of feature extraction.

Ideally, the tissue region should be at a fixed location in the image. This would make it possible to crop all images in a given column at the same position, given the tissue width. However, this is not always the case. In case of interruptions in the imaging process like power outages and clogging in the water circulation, the KESM might need to be stopped for maintenance and the setup might be disturbed. In such scenarios, after restarting the KESM, the start of tissue may not be at the same pixel position in the image as before. In this case, cropping at fixed position may cause loss of tissue data. This necessitates detection of the tissue edge for every image.

Each tissue sample imaged by the KESM can generate up to around 80,000 images (the tissue is laterally sectioned several times and each column has around 10,000 images). Thus, to extract tissue region

manually requires a lot of time and effort and is inefficient. So we need image processing to automate this. A template matching based method was proposed for tissue extraction from the KESM image stacks (Kwon et al., 2011). However, this method suffered from a high error rate. The novel algorithm for tissue extraction proposed in this paper has lower error rates and is more efficient in automation of the process.

Knife chatter and illumination artifacts affect KESM images as shown in Figure 9. Varying cutting speeds introduced to reduce knife chatter cause inter-image intensity differences. These artifacts hinder visualization and feature extraction. So inter- and intra- image normalization is also a necessary preprocessing step for KESM stacks.

## 3 METHOD

This section explains the newly proposed tissue area detection and extraction algorithm. It focuses on the reasoning behind the methodology used. We also describe the method used for intensity normalization algorithm as proposed in (Kwon et al., 2011) for completeness.

### 3.1 Tissue Area Detection

The image from the KESM consists of a right and a left edge of tissue as shown in Figure 2(a). Figure 2(b) shows the seemingly sharp right-edge. However, Figure 2(c) reveals gradual decay in the intensity profile of the right edge. Moreover, KESM is affected by multiple artifacts as described earlier. For this reason, we do not use the Sobel (Duda et al., 1973), Prewitt (Prewitt, 1970) and similar edge detectors. The Canny edge detector (Canny, 1986) is robust to noise (Maini and Aggarwal, 2009) but is complex to compute and gives us additional information about corners that we do not need. Hence, we take the Gaussian gradient, which can smooth the image before detecting edge gradients to give us a clear right edge location. The Gaussian Gradient applies a filter in the  $x$  and  $y$  directions of the two dimensional tissue image being processed. The equations for first order Gaussian derivatives of Gaussian are as given below:

$$\frac{dG(x,y,\sigma)}{dx} = \frac{-x}{2\pi\sigma^4} e^{-\frac{(x^2+y^2)}{2\sigma^2}} \quad (1)$$

$$\frac{dG(x,y,\sigma)}{dy} = \frac{-y}{2\pi\sigma^4} e^{-\frac{(x^2+y^2)}{2\sigma^2}} \quad (2)$$

,where  $x$  and  $y$  represent the kernel location starting with zeros at the center and  $\sigma$  represents the standard

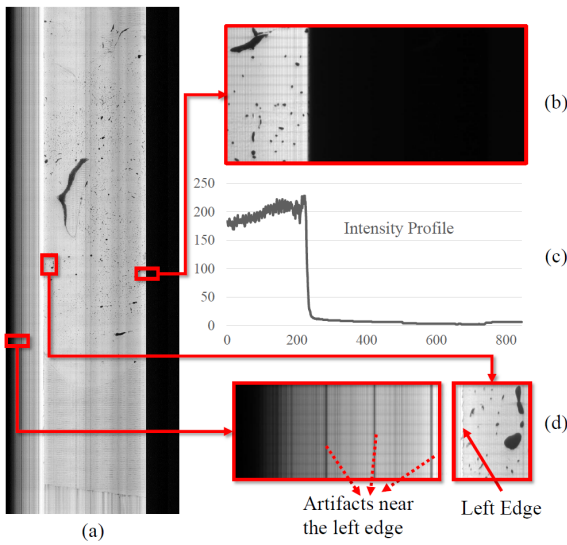


Figure 2: Showing the spurious data and edges of tissue region in image. (a) One Tissue Slice from KESM microvasculature data stack. (b) Right Edge of Tissue expanded shows sharp demarcation. (c) Intensity Profile along x axis (distance in pixels from the left side of the image shown in (b)) shows a gradual gradient that might cause spurious edge detection by some edge operators. (d) Left edge (the solid arrow) of tissue expanded shows vertical noise lines (dotted arrows) that have to be distinguished from the real left edge.

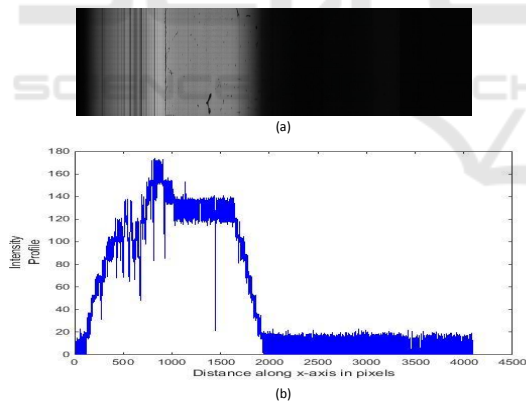


Figure 3: A horizontal section from a KESM image with no clear right edge necessitating left edge detection. (a) A small horizontal section of KESM image with occluded right edge. (b) Intensity profile along the x axis of the image shown in (a)

deviation of the Gaussian distribution. Smoothing effect of the Gaussian Kernel, increases as  $\sigma$  increases.

This algorithm does not work with right-occluded images. Figure 3 shows a horizontal section from a KESM image with no clear right edge. It is seen that the edge like profile occurs much before the actual image edge. In these cases we try to detect the left edge of tissue to crop the image. It is challenging due

to vertical noise artifacts produced by illumination irregularities in the KESM shown in Figure 2(d).

The technique used to find the left edge relies on the fact that in KESM images, only the correct left edge has more horizontal as well as vertical gradients. To use this information efficiently, we first take the horizontal followed by the vertical Gaussian gradient of the image. This leaves us with a strong response at the left edge. We then use a thresholding to eliminate the weak responses of vertical noise outside the left tissue edge. Then, the image is optionally eroded with a slightly elongated rectangular structuring element to strengthen edges that remain.

To detect the position of the strong vertical response from this image, we use probabilistic hough line (Galamhos et al., 1999) estimation with one single angle (zero) and a decreasing line length starting from half the height of the entire image. The location of the longest vertical line found in the left half of the image is taken to be the index of the left edge.

Rarely, a KESM image is so dark that neither the left edge nor the right edge of the tissue can be reliably found by the proposed algorithm. Our effort to make the image processing pipeline fully automated involved using a best-effort thresholding based tissue region detection algorithm. Minimum cross entropy approach has proven to be a useful segmentation method in many applications and it has been used in (Yi-de et al., 2004; Sarkar et al., 2011; Al-Attas and El-Zaart, 2007) efficiently, which is empirical evidence for effectiveness of this threshold. So in our algorithm, we used Li threshold (Li and Lee, 1993) that is based this thresholding. Thus the proposed automated algorithm will extract the tissue region from every single image generated by the KESM, with best-effort cropping for very occluded or dark images.

### 3.2 Image Intensity Normalization

We implemented the image intensity equalization algorithm previously proposed for KESM image stacks (Kwon et al., 2011). Briefly, this method normalizes each pixel in a row or column based on the median intensity value of that row or column. This procedure is applied to all rows and columns in the image to achieve uniform intensity. We also adopt the method of selective normalization and set a threshold for foreground segmentation when the median intensity is too low to get a clear distinction between tissue and background. It alleviates artifacts and translates all images to a common background intensity level.

## 4 IMPLEMENTATION

The algorithm for tissue extraction developed in this paper consists of three logical divisions - edge detection, admissibility check and cropping. Edge is detected using one of the two methods explained below or by thresholding based right edge detection. The overview of the algorithm flow is shown in Figure 4. Once the tissue region is extracted from the image, a normalization algorithm is applied to enable further processing. The interested reader is referred to (Kwon et al., 2011) for the implementation details.

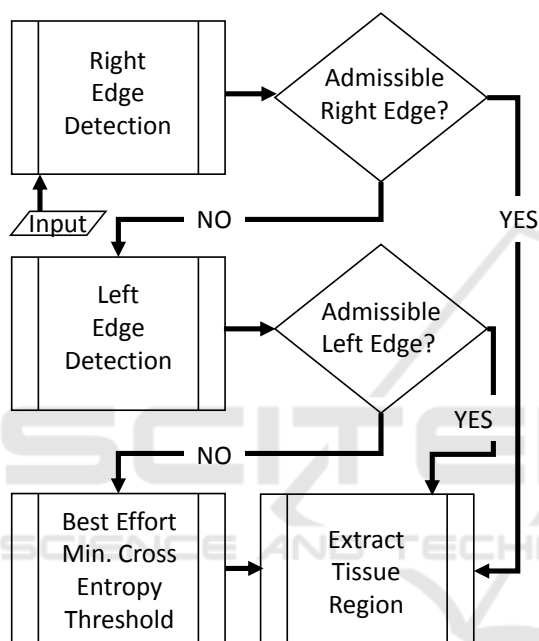


Figure 4: Flowchart showing the logical structure of proposed automated cropping algorithm

### 4.1 Right Edge Detection for Tissue Extraction

The right edge detection algorithm involves finding the right edge at the strongest Gaussian gradient re-

**Algorithm 1:** Right Edge Detection.

```

1: function FIND_RIGHT_EDGE
2:   init
3:   image ← image *  $\frac{dG(x,y,2)}{dx}$ 
4:   image ← image *  $\frac{dG(x,y,2)}{dy}$ 
5:   y,x ← Non-zero Indices from image
6:   xo ← (val,occ) in x,sorted by freq. of val
7:   x ← xo for 10 highest "val" in xo
8:   index ← val with max(occ) x
9:   return index
    
```

sponse on the right half of image. The Gaussian gradient function with sigma of 2 is applied. First, the horizontal derivative of Gaussian is convolved with the image (convolution is indicated by  $*$ ) and then the result is convolved with vertical derivative of Gaussian. Ideally, this gives an image with its last non-zero pixel along the x-axis at the right edge of tissue in the image. However, to ensure the algorithm is picking the most well defined edge, the largest non-zero x-index (val) that corresponds most occurrences (occ) of non-zero pixels in y is chosen as the result. The pseudo-code for this procedure is given in Algorithm 1. This works for any KESM image that has sufficient contrast at the right edge. However, if the right edge of tissue is too dark or blurred to recover due to artifacts introduced by the imaging mechanism, this will not give the correct right edge location. The result provided by this right edge detection function is validated by an admissibility test based on tissue width (TissueWidth), sanity checks and image properties near detected edge. If the result is admissible, it is used to crop the tissue from [index-TissueWidth,index]. If not, the left edge detection algorithm, described next, is used to try and find the index of the left edge of tissue region.

### 4.2 Left Edge Detection for Tissue Extraction

The left edge detection algorithm works by isolating the edge with greater vertical connectivity and also maximum horizontal gradients on the left half of the image. The Gaussian gradient works with lesser smoothing than for right edge detection. This is to ensure we do not smooth out the gradient information we are trying to detect on the left edge. After this edge

**Algorithm 2:** Left Edge Detection.

```

1: function FIND_LEFT_EDGE
2:   init
3:   image ← image *  $\frac{dG(x,y,1)}{dx}$ 
4:   image ← image *  $\frac{dG(x,y,1)}{dy}$ 
5:   image ← Triangle thresholded image
6:   image ← BinaryErode(image)
7:   roi_lines ← WIDTH - TissueWidth
8:   image ← image[0:roi_lines]
9:   while lines == [ ] and height ≠ 0 do
10:    lines ← hough_lines(image,height)
11:    height ← height - predefined_dec_step
12:   if lines == [ ] then
13:     return fail
14:   index ← x_inx of longest line found
15:   return index
    
```

detection step, we apply a triangle threshold to binarize the image. This image is then given as an input to a binary erode filter using a narrow rectangular structuring element. This ensures that only the strongest vertical lines survive. Then probabilistic hough lines are found in the y-direction and the highest connected vertical line which in turn is the tallest line found is taken as being at the position of the left edge. The x-index at which this line was found is returned to the cropping algorithm. The pseudo-code for this procedure is given in Algorithm 2.

If the left edge found is admissible, tissue region is extracted with the result index value. If not, the image is cropped with a best effort algorithm based on minimum cross entropy threshold (Li and Lee, 1993). The image is first thresholded based on this method. Then the strongest vertical edge in the image that is farthest to the right is taken as the right edge of the tissue region.

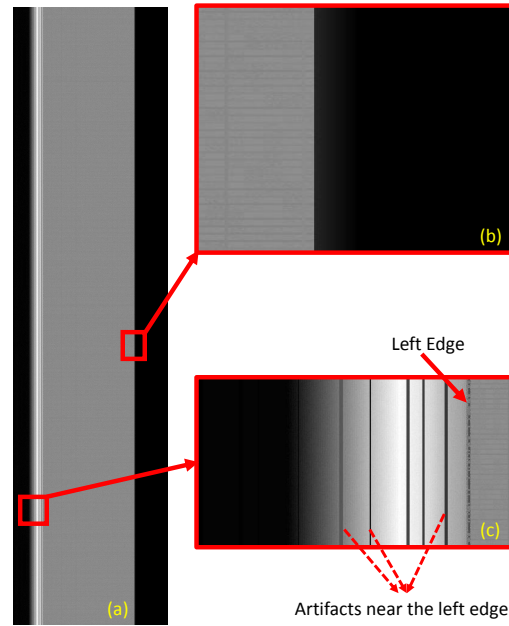


Figure 5: Synthetic image. It has edge properties that mimic the real KESM images. These images can thus serve as ground truth for validation of results from the proposed algorithm. (a) Full synthetic image. (b) Right edge magnified. (c) Left edge magnified.

## 5 VALIDATION

Validation with a real data subset is impractical because we have to manually find the correct tissue edge in each image. This would be subjective, error prone and cannot be considered ground truth. So the proposed algorithm was validated using synthetic images. The algorithm was run on a computer with an AMD-64 quad-core processor running at 3.8GHz with 8GB RAM.

### 5.1 Testing Proposed Algorithm

The tissue extraction code itself that was explained in the implementation section was written in Python. The code for normalization of the data was written in C++. Synthetic images were generated using a python script. They mimic the properties of KESM images and their artifacts. They faithfully reproduce the nature of the edges of tissues in KESM data. An example of an image generated by this algorithm is shown in Figure 5(a). The edge properties are shown in Figure 5(b) and (c). Thus, we can assume that the results from the synthetic data are directly representative of those from KESM data. We tested the proposed cropping algorithm on hundred synthetic images. From this, the average and maximum errors were found to be 2.68 pixels and 7 pixels respectively.

### 5.2 Comparative Evaluation

We also compared the proposed method to a previously proposed algorithm for tissue extraction. The algorithm being compared is the template matching(TM) based cropping algorithm proposed in (Kwon et al., 2011). Error in the number of pixels for both these methods is compared in the chart shown in Figure 6. From this we infer that the proposed algorithm has improved error rate by 90.92% compared to the template matching based algorithm. The minimum error for the template matching based algorithm for the same set of synthetic images is 15 pixels whereas the proposed algorithm is capable of

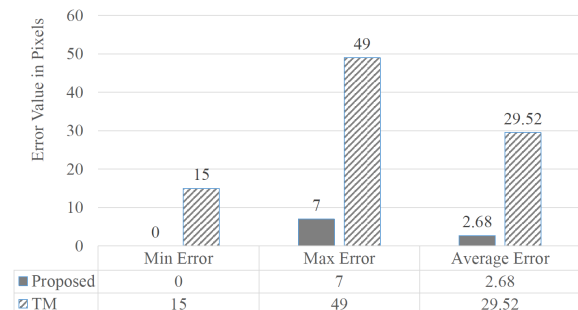


Figure 6: Quantitative comparison between the proposed algorithm for tissue extraction and the template matching algorithm from (Kwon et al., 2011).

cropping images with zero error. Figure 7 shows the result of cropping using the two methods on a synthetic image. Clearly, the proposed algorithm has better accuracy in locating the edge of tissue region in the image.

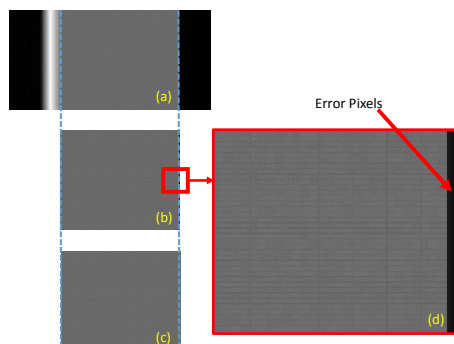


Figure 7: Comparison of cropping using proposed method and template matching method on a synthetic image for qualitative results. (a) A small horizontal portion from a synthetic image. Right edge location =  $3442(x)$ . (b) Output of template matching algorithm proposed in (Kwon et al., 2011). (c) Output of proposed algorithm cropped at  $3442(x)$  with zero error. (d) Magnified result from the rectangle shown in (b) indicating erroneous pixels near the right edge after cropping, crop location =  $3459(x)$ .

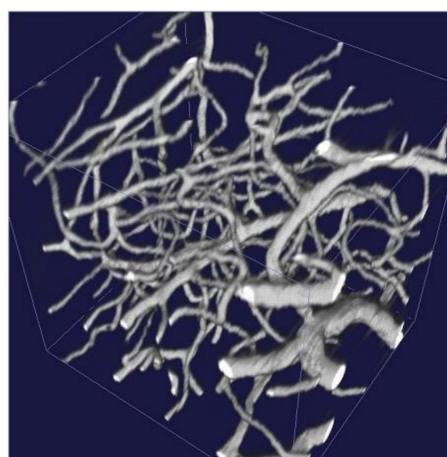
## 6 REPRESENTATIVE RESULTS

We ran the proposed cropping algorithm on the mouse brain vasculature data stacks imaged by the KESM. We could crop the entire image stack and also normalize all the images after cropping. This method was robust enough to work on very dark, very bright and images affected by different artifacts that are common in KESM including illumination artifacts. This can be seen in Figure 9. Each of the figures show the original, cropped and normalized versions of the KESM images that have been affected by different artifacts.

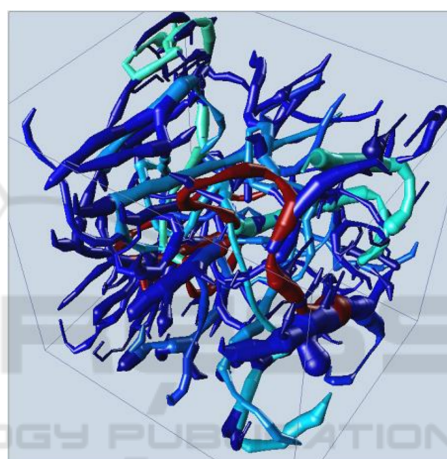
The traced result shown in Figure 8 was generated using the All Path Pruning 2.0 (APP2) (Xiao and Peng, 2013) plug-in in Vaa3D (Peng et al., 2010). Default APP2 parameters were used for the trace except the *background\_threshold* that was set to  $-1$ . The KESM image stack was inverted to have a bright foreground tissue area on a dark background.

## 7 CONCLUSION AND FUTURE WORK

A new algorithm has been proposed to extract tissue region from physical sectioning based light mi-



(a)



(b)

Figure 8: 3D visualization of the image data. (a) 3D view of a properly cropped image volume using the proposed algorithm. The dimension of the image is  $153 \times 179 \times 177$  scaled by  $0.6 \times 0.7 \times 1.0$  ratio (b) A blood vessel trace result of (a) using the Vaa3D (Peng et al., 2010) plugin based on the All Path Pruning 2.0 (APP2) algorithm (Xiao and Peng, 2013).

croscopy image stacks. The algorithm was developed using the mouse brain vasculature data set generated by the KESM. The challenges were mainly the varying nature of KESM images, which the algorithm was designed to handle. This made it possible to crop the entire image stack automatically with high accuracy. The average error for the proposed method was found to be less than 3 pixels from tests on synthetic data. This was compared against a previously proposed method for tissue extraction and quantitative comparison results have been shown in the paper. This algorithm along with normalization, is part of preprocessing.

An image processing pipeline of our design is proposed as shown in Figure 10. The goal is to automat-

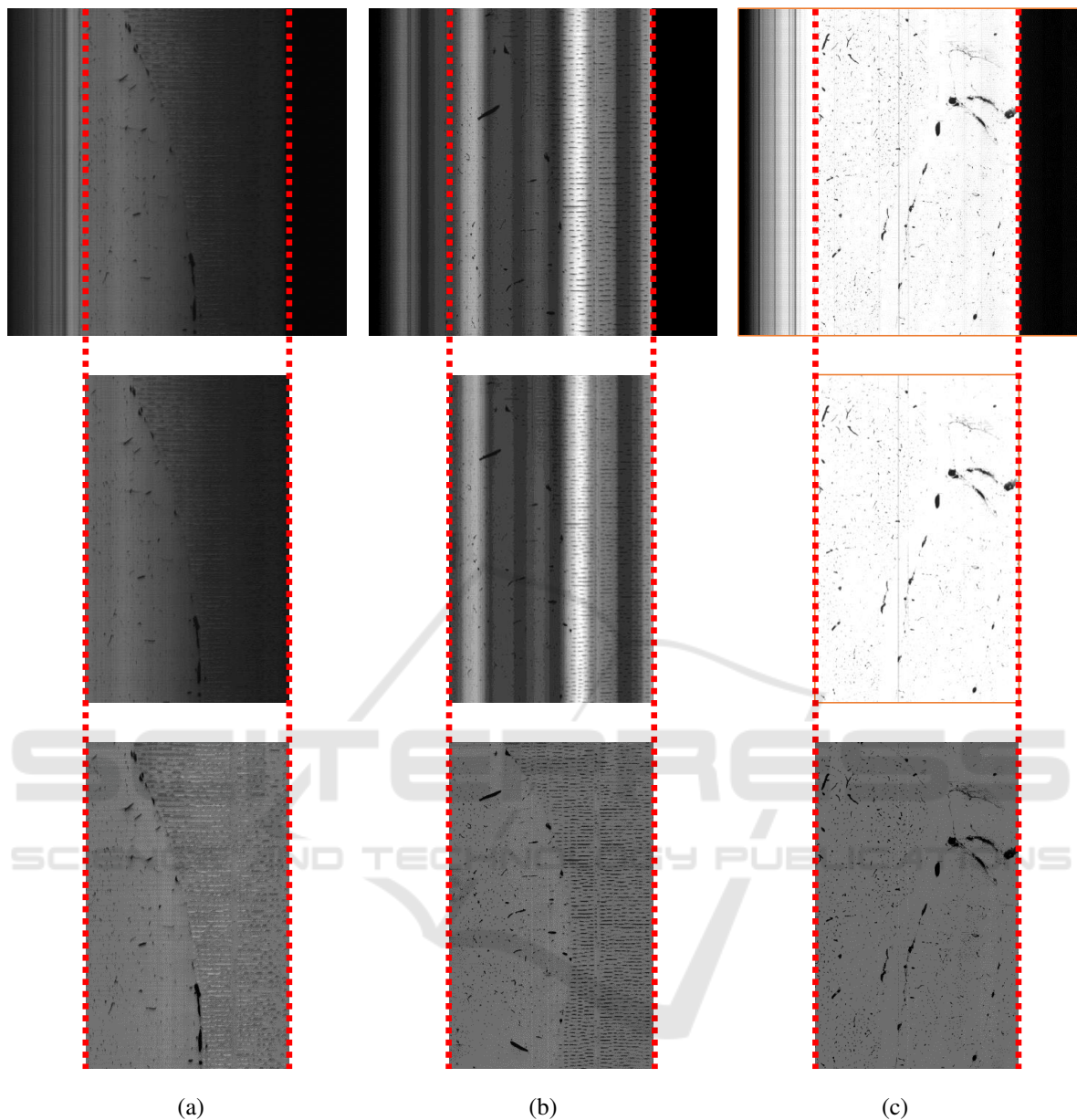


Figure 9: Results of proposed algorithm to find tissue edge under different conditions and the output of normalization algorithm. A small portion from a sample KESM image (top row). The image cropped using proposed tissue extraction algorithm (middle row). Image normalized using algorithm adapted from (Kwon et al., 2011) (bottom row). (a) A very dark KESM image (brightness increased for viewing only), the extracted tissue region and its normalized version. (b) A KESM image with severe illumination artifacts in the form of vertical bands that could be mistaken for edges, the extracted tissue region and its normalized version. (c) A very bright KESM image, the extracted tissue region and its normalized version.

ically extract the important biological features from light microscopy images and also publish it online for the scientific community to access.

## ACKNOWLEDGEMENTS

This material is based upon work supported by the National Science Foundation (NSF) #1337983.

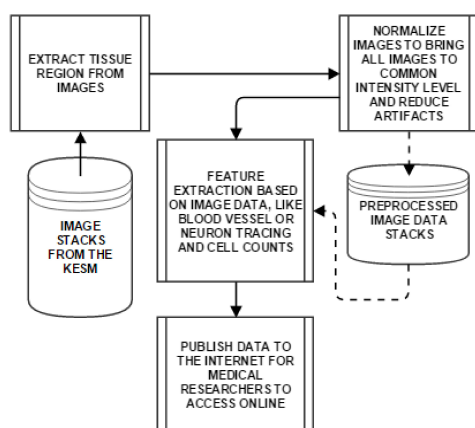


Figure 10: A pipeline to be implemented for information extraction from the KESM and other physical sectioning-based microscope image stacks

## REFERENCES

- Al-Attas, R. and El-Zaart, A. (2007). Thresholding of medical images using minimum cross entropy. In *3rd Kuala Lumpur International Conference on Biomedical Engineering 2006*, pages 296–299. Springer.
- Canny, J. (1986). A computational approach to edge detection. *Pattern Analysis and Machine Intelligence, IEEE Transactions on*, (6):679–698.
- Choe, Y., Mayerich, D., Kwon, J., Miller, D. E., Sung, C., Chung, J. R., Huffman, T., Keyser, J., and Abbott, L. C. (2011). Specimen preparation, imaging, and analysis protocols for knife-edge scanning microscopy. (58):e3248.
- Denk, W. and Horstmann, H. (2004). Serial block-face scanning electron microscopy to reconstruct three-dimensional tissue nanostructure. *PLoS Biol*, 2(11):e329.
- Duda, R. O., Hart, P. E., et al. (1973). Pattern classification and scene analysis. *J. Wiley and Sons*.
- Galamhos, C., Matas, J., and Kittler, J. (1999). Progressive probabilistic hough transform for line detection. In *Computer Vision and Pattern Recognition, 1999. IEEE Computer Society Conference on*, volume 1. IEEE.
- Hayworth, K., Kasthuri, N., Schalek, R., and Lichtman, J. (2006). Automating the collection of ultrathin serial sections for large volume tem reconstructions. *Microscopy and Microanalysis*, 12(S02):86–87.
- Kwon, J., Mayerich, D., and Choe, Y. (2011). Automated cropping and artifact removal for knife-edge scanning microscopy. In *Biomedical Imaging: From Nano to Macro, 2011 IEEE International Symposium on*, pages 1366–1369. IEEE.
- Li, C. H. and Lee, C. (1993). Minimum cross entropy thresholding. *Pattern Recognition*, 26(4):617–625.
- Maini, R. and Aggarwal, H. (2009). Study and comparison of various image edge detection techniques. *International journal of image processing (IJIP)*, 3(1):1–11.
- Mayerich, D., Abbott, L., and McCormick, B. (2008). Knife-edge scanning microscopy for imaging and reconstruction of three-dimensional anatomical structures of the mouse brain. *Journal of microscopy*, 231(1):134–143.
- Peng, H., Ruan, Z., Long, F., Simpson, J. H., and Myers, E. W. (2010). V3d enables real-time 3d visualization and quantitative analysis of large-scale biological image data sets. *Nature biotechnology*, 28(4):348–353.
- Prewitt, J. M. (1970). Object enhancement and extraction. *Picture processing and Psychopictorics*, 10(1):15–19.
- Sarkar, S., Patra, G. R., and Das, S. (2011). A differential evolution based approach for multilevel image segmentation using minimum cross entropy thresholding. In *Swarm, Evolutionary, and Memetic Computing*, pages 51–58. Springer.
- Shotton, D. M. (1989). Confocal scanning optical microscopy and its applications for biological specimens. *Journal of Cell Science*, 94(2):175–206.
- Tsai, P. S., Friedman, B., Ifarraguerra, A. I., Thompson, B. D., Lev-Ram, V., Schaffer, C. B., Xiong, Q., Tsien, R. Y., Squier, J. A., and Kleinfeld, D. (2003). All-optical histology using ultrashort laser pulses. *Neuron*, 39(1):27–41.
- Xiao, H. and Peng, H. (2013). App2: automatic tracing of 3d neuron morphology based on hierarchical pruning of a gray-weighted image distance-tree. *Bioinformatics*, 29(11):1448–1454.
- Yi-de, M., Qing, L., and Zhi-Bai, Q. (2004). Automated image segmentation using improved pcnn model based on cross-entropy. In *Intelligent Multimedia, Video and Speech Processing, 2004. Proceedings of 2004 International Symposium on*, pages 743–746. IEEE.